Spring 2015

A bracketing method for proton affinity measurements of dehydro-and didehydropyridines

Guannan Li
Purdue University

A BRACKETING METHOD FOR PROTON AFFINITY MEASUREMENTS OF DEHYDRO- AND DIDEHYDROPYRIDINES

A Thesis

Submitted to the Faculty

of

Purdue University

by

Guannan Li

In partial Fulfillment of the

Requirements of the Degree

of

Master of Science

May, 2015

Purdue University

West Lafayette, Indiana

To my loving parents, Jiaxin Li and Wei Zhang

ACKNOWLEDGMENTS

First of all, I would like to thank my advisor Dr. HilkkaKenttamaa for giving me the opportunity to work in this group and support me during my time in Purdue. I have been trained on different types of mass spectrometers in the group and also learned many useful techniques in lab. What's more, I was always inspired by Dr. HilkkaKenttamaa's passion for chemistry and admired her humbleness and kindness as a person.

I would also like to thank Dr. John Nash, who did all the calculations in this work. Without his calculations, I wouldn't complete this work as I did now.

Many thanks to everyone who I enjoyed working with, including Linan Yang, Vanessa Gallardo,Ben Owen, Fanny Widjaja, Sabir Aqueel, Peggy Williams, Jinshan Gao, James Riedeman, Huaming Sheng, Weijuan Tang, ChunfenJin, Hanyu Zhu, PriyaMurria and other former and present group members.

Last but not least, I would like to thank my parents for supporting me during this program, for your deep love and understanding.

TABLE OF CONTENTS

Page

LIST OF TABLES vi

LIST OF FIGURES vii

LIST OF SCHEMES viii

ABSTRACT ix

CHAPTER 1: INTRODUCTION AND OVERVIEW 1

1.1 Introduction 1
1.2 Overview 1
1.3 References 3

CHAPTER 2: INTRUMENTAL AND EXPERIMENTAL ASPECTS AND THEORY OF FOURIER TRANSFORM ION CYCLOTRON (FT-ICR) MASS SPECTROMETER 4

2.1 Introduction 4
2.2 Ionization Methods 5
2.2.1 Electron Ionization (EI) 5
2.2.2 Chemical Ionization (CI) 6
2.3Fourier-Transform Ion Cyclotron Resonance (FT-ICR) Mass Spectrometer 7
2.3.1 FT-ICR Instrumentation 7
2.3.2 Ion Motion in FT-ICR 10
2.3.3 Ion Generation 14
2.3.4 Ion Transfer from Source Cell Into Analyzer Cell 14
2.3.5Ion Excitation and Detection 15
2.3.6Ion Isolation 17
2.3.7 Collision-Activated Dissociation (CAD) 18
2.4 References 20

Page

CHAPTER 3: A BRACKETING METHOD FOR PROTON AFFINITY (PA) MEASUREMENTS OF DEHYDRO- AND DIDEHYDROPYRIDINES 22

3.1 Introduction.....22
3.2 Experimental Details.....24
3.3 Measured Proton Affinities of Dehydro- and Didehydropyridines 28
3.4 Comparison of Calculated and Experimental Proton Affinity Values.....34
3.5 Conclusions.....37
3.6 References.....39

LIST OF TABLES

Tables Page

3.1 The Lowest Detectable Endothermicity was Measured to be 1.6 kcal/mol by Observing the Occurrence of Proton Transfer Reaction between Three Pairs of Reference Bases with Known Proton Affinities 27

3.2 Proton Affinities of 2-, 3- and 4-Didehydropyridines Measured by Observing the Occurrence of Exothermic Proton Transfer Reactions with Reference Bases 30

3.3 Proton Affinities of 2,3-, 2,4-, 2,5-, 2,6-, 3,4- and 3,5-Didehydropyridines Measured by Observing the Occurrence of Exothermic Proton Transfer Reactions with Reference Bases 32

3.4 Comparison of Calculated and Experimental PAs of the Radicals and Biradicals 35

LIST OF FIGURES

Figure Page

2.1 Schematic of the dual cell FT-ICR mass spectrometer used in this research 8

2.2 The source cell (left) and analyzer cell (right) are divided by the conductance limit. The excitation and detection plates are perpendicular to the magnetic field, and the trapping plates are parallel to the magnetic field. 9

2.3 The cyclotron motion of a positive ion in the x-y plane perpendicular to the magnetic field.....11

2.4 Cyclotron and trapping motions of an ion in an ICR cell 12

2.5 All three motions of ions in an ICR cell: cyclotron motion (orange), trapping motion (red), and magnetron motion (blue). The magnetron motion radius is greatly exaggerated comparing to the cyclotron motion in order to show them in the same figure.....13

2.6 Illustration of ion excitation and detection. An rf pulse is applied to the excitation plates to increase the radius of ion cyclotron motion (left, excitation), and the induced image current is detected by the detection plates (right, detection).....16

3.1 Flow chart of the experiment, starting with the generation of protonated 2-dehydropyridine and transfer into another cell followed by SORI-CAD, cooling, and reaction with a reference base. 26

3.2 Structures of the 2,5-didehydropyridium cation (left) and its enediyne isomer (right) 36

LIST OF SCHEMES

Scheme Page

2.1 Electron ionization 6

2.2 Self Chemical ionization 7

3.1 Definition of proton affinity 23

ABSTRACT

Li, Guannan. M.S., Purdue University, May, 2015. A Bracketing Method for Proton Affinity Measurements of Dehydro- and Didehydropyridines. Major Professor: HilkkaKenttämaa.

Proton affinity (PA) is a fundamental property that is related to the structure and reactivity of a molecule. Currently, very few experimental PA values are available for organic radicals and none for biradicals. Equilibrium methods cannot be used for these measurements. The traditional bracketing method is based on monitoring reactions of different reference bases with known proton affinities with the protonated analyte for the occurrence of exothermic proton transfer to determine the upper and lower limits of proton affinity. However, the energy deposited into the precursor ions upon CAD when forming protonated radicals may cause endothermic proton transfer reactions occur albeit slowly. Their occurrence limits the accuracy of the measurement. The bracketing method was modified to allow distinction between exothermic and slightly endothermic proton transfer reactions. This method was used to measure the PA values for three dehydropyridine radicals and six didehydropyridinebiradicals. The values were compared to those obtained using quantum chemical calculations.

CHAPTER 1: INTRODUCTION AND OVERVIEW

1.1 Introduction

Aromatic mono- and biradicals have received more attention in recent years because of the importance of these reaction intermediates in many fields, including organic synthesis and biological activity of organic compounds.[1,2,3] In the study of the reactivities of charged radicals towards different neutral organic molecules, the acidities of the charged radicals (or proton affinities (PA) of their conjugate bases) have been found to be one of the variables that need to be considered.[4] It is a fundamental property that is related to the structure and reactivity of a molecule/radical. However, very few experimental PA values are available for organic radicals and none for biradicals. Therefore, in this work, a modified bracketing method was developed to measure the proton affinities of mono- and biradicals.

1.2 Overview

This thesis consists of three chapters describing the study and utilization of a bracketing method for the measurement of proton affinities (PA) of pyridine based mono-

and biradicals. Since all the experiments performed in this work utilized a Fourier transform ion cyclotron resonance (FT-ICR) mass spectrometer, Chapter 2 provides a brief introduction to the fundamental principles of FT-ICR mass spectrometers.

Chapter 3 describes proton affinity measurements using a modified bracketing method and a FT-ICR mass spectrometer and the comparison of experimental results and calculations.

1.3 References

1. Wolf, C.; Tumambac, G. E.; Villalobos, C. N. *Synlett.* **2003**, 1801.

2. Zoltewicz, J. A.; Maier, N. M.; Lavieri, S.; Ghiviriga, I.; Abboud, K. A.; Fabian, W. M. F. *Tetrahedron* **1997,** *53*, 5379.

3. Griffith, J.; Murphy, J. A. *J. Chem. Soc. Chem. Commun.* **1992**, *1*, 24.

4. Jankiewicz, B. J.;Kenttämaa, H. I.*J. Phys. Org. Chem*. **2013**, *26*, 707.

CHAPTER 2:
INSTRUMENTAL AND EXPERIMENTAL ASPECTS AND THEORY OF FOURIER TRANSFORM ION CYCLOTRON (FT-ICR) MASS SPECTROMETER

2.1 Introduction

Over the last several decades, mass spectrometry (MS) has developed rapidly and become one of the most powerful techniques used in fields such as biotechnologyand pharmaceutical, environmental and clinical analyses,[1] as well as determination of properties of reactants and reaction intermediates.[2]

Basic steps of mass spectrometric analysis are evaporation of analytes, analyte ionization, separation of ions by their mass-to-charge ratios, and detection of ions. Besides these basic analysis steps, ion-molecule reactions can also be performed using some mass spectrometers to obtain thermochemical properties of aimed analytes. For the experiments in this dissertation, a 3-Tesla Finnigan Model FTMS 2001 Fourier transform ion cyclotron resonance (FT-ICR) mass spectrometer was utilized to measure and investigate the proton affinities of highly reactive pyridine based monoradicals and biradicals.

The principles of FT-ICR mass spectrometers have been discussed in great detail in the literature.[3,4,5,6]In this chapter, some fundamental and experimental aspects of this instrument are briefly discussed.

2.2 Ionization Methods

Ionization is a critical step in mass spectrometric analysis. The analytes need to have a charge to be manipulated in the magnetic and electric fields in a mass spectrometer. Many different ionization methods have been developed, each of them with its advantages and disadvantages. The choice of an ionization method usually depends on the natural properties of the analytes and also by the desirable information. In this dissertation, two ionization methods which have been used in the experiment on FT-ICR are discussed; they are electron ionization (EI) and chemical ionization (CI).

2.2.1 Electron Ionization (EI)

Electron ionization, also known as electron impact ionization, introduced in early 20th century is one of the oldest ionization methods.[7] In EI, analyte molecules are bombarded by a stream of energetic electrons in the gas phase. The collision between an electron and the neutral analyte molecule can result in the ejection of an electron from the analyte molecule to form the molecular ion[8,9] (Scheme 2.1). If the internal energy of the

molecular ion exceeds the fragmentation threshold, fragments are observed. Since the fragmentation patterns are reproducible, EI mass spectra provide useful information in compound identification.

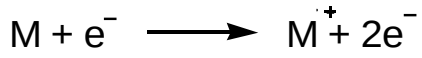

Scheme 2.1 Electron ionization

2.2.2 Chemical Ionization (CI)

Chemical ionization (CI) generates ions via collisions between neutral molecules and the chemical ionization reagent ions.[10,11,12] Compared to EI, CI is a "soft" ionization technique. By using CI, fewer fragments form during the process which makes it possible to get molecular weight information for the analyte molecules. In this work, self-CI was used to ionize the radical precursor molecules. Self-CI begins with EI of the analyte, followed by abstraction of a hydrogen atom from the neutral analyte molecule, resulting in the formation of a protonated analyte. (Scheme 2.2)

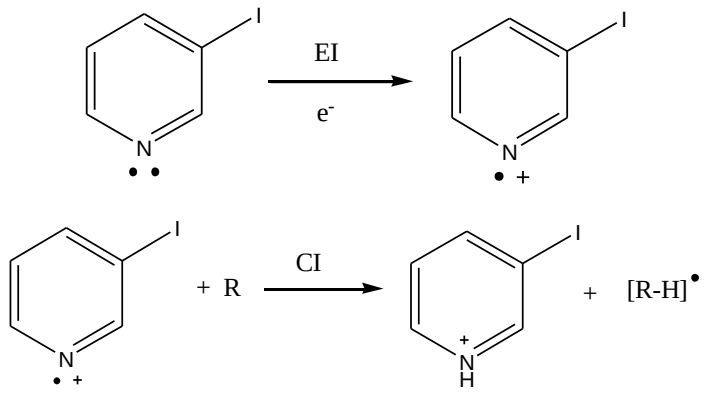

Scheme 2.2Self chemical ionization

2.3 Fourier-Transform Ion Cyclotron Resonance (FT-ICR) Mass Spectrometer

2.3.1 FT-ICR Instrumentation

FT-ICR is a combination of FT and ICR techniques. It is known as a high resolution and high mass accuracy mass spectrometer.[5] In addition, FT-ICR is capable of multistage MS/MS experiments and can be used with several ionization methods.[13,14,15]

In this thesis, all the experiments were carried out in a dual-cell Finnigan Model 2001 Fourier-transform ion cyclotron resonance mass spectrometer (FT-ICR, Figure 2.1) equipped with a Sun Sparc 20 data station running Odyssey version 4.0 software.[16] Two Edward 160P/700 (800 L s^{-1}) diffusion pumps (one for each cell) were used to maintain a high vacuum with a nominal base pressure lower than 10^{-9}torr. Two Alcatel

mechanical pumps were used to back up the two diffusion pumps. The pressure of each cell was measured by using two Bayard-Alpert ionization gauges located on each side of the dual cell.[17]

This instrument had several inlets for introduction of different types of compounds into the mass spectrometer. The analytes can be gases, liquids and solids. Pulsed valves were used to introduce gases and volatile liquids. Batch inlets were used to introduce volatile liquidsa and Varian leak valves for nonvolatile liquids and volatile solids. Solids probes were used for nonvolatile solid compounds.[18,19]

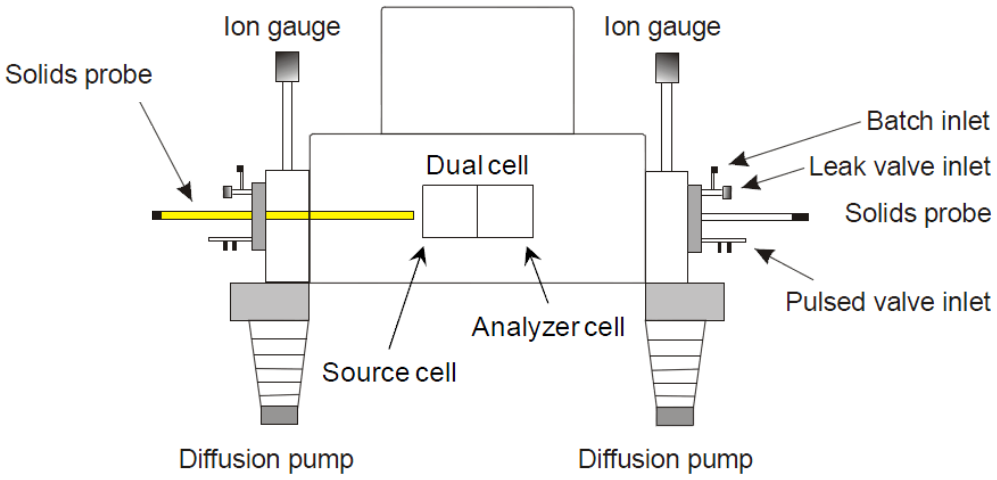

Figure 2.1 Schematic of the dual cell FT-ICR mass spectrometer used in this research

The main component of this instrument is the dual-cell. It is composed of two identical

cubic cells (4.763 cm^3 each) (Figure 2.2). Ions are stored, manipulated and detected in the cells. This dual-cell is positioned in the center of the vacuum chamber of the FT-ICR, and it's aligned with the magnetic field. The two cells shared a common plate called the conductance limit with a 2-mm hole in the center.[20]The two plates at the two ends of the cells are called trapping plates. The plates at top and bottom are called detection plates; the two remaining plates are called excitation plates. The two trapping plates are maintained at +2 V in the instruments and the conductance limit is grounded during transfer event, otherwise it's at the same voltage as the two trapping plates.

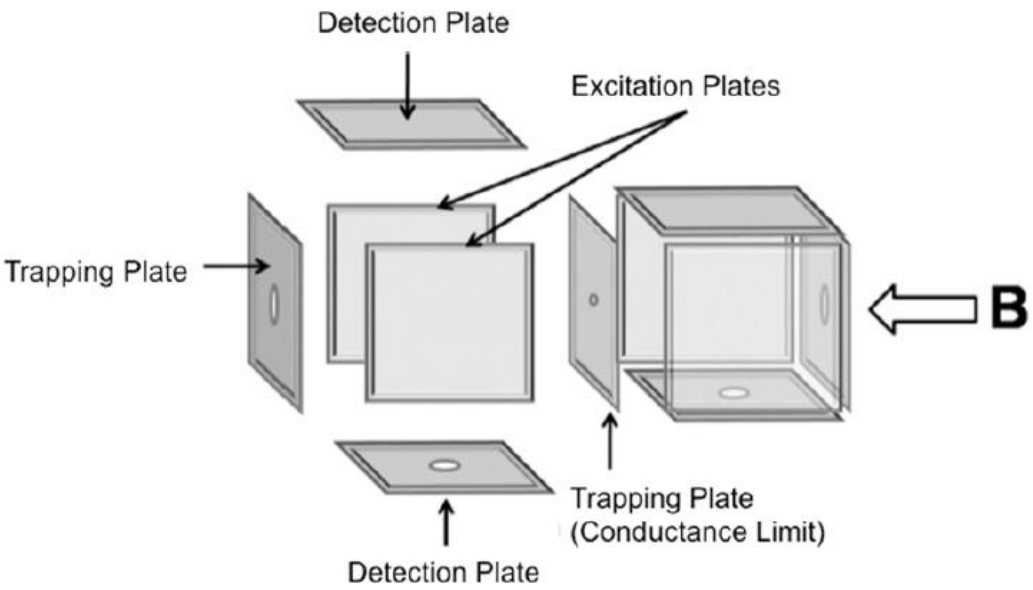

Figure 2.2 The source cell (left) and analyzer cell (right) are divided by the conductance limit. The excitation and detection plates are perpendicular to the magnetic field, and the trapping plates are parallel to the magnetic field

2.3.2 Ion Motion in FT-ICR

Ion motion in an FT-ICR mass spectrometer is governed by magnetic and electric fields.[5] Three basic motions observed on FT-ICR are: cyclotron motion, trapping motion and magnetron motion.[21]

In a uniform magnetic field, a moving ion is subjected to the Lorentz force, $F_{Lorentz}$, as described by the following equation:

$$F_{Lorentz} = qv \otimes B \qquad (2.1)$$

In this equation, q, v and B are the charge of the ion, the velocity of the ion and the magnetic field strength, respectively.[5,22] The Lorentz force is counterbalanced by the centrifugal force, $F_{Centrifugal}$, as described by the following equation:

$$F_{Centrifugal} = \frac{mv^2}{r} \qquad (2.2)$$

When an ion is moving in a stable manner on a circular orbit, Lorentz force is equal to centrifugal force (Figure 2.3). Equation 2.3 is obtained by combining equation 2.1 and equation 2.2:

$$qvB = \frac{mv^2}{r} \qquad (2.3)$$

Rearranging equation 2.3 gives:

$$\frac{qB}{m} = \frac{v}{r} \quad (2.4)$$

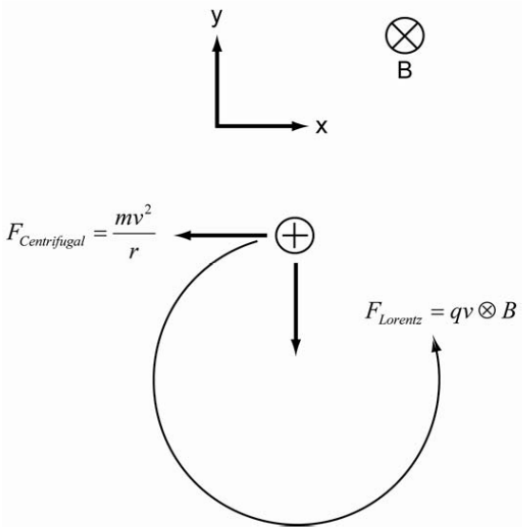

Figure 2.3 The cyclotron motion of a positive ion in the x-y plane perpendicular to the magnetic field

The relationship between cyclotron frequency (ω_c) of an ion and velocity and radius of the motion is shown in following equation:

$$\omega_c = \frac{v}{r} \qquad (2.5)$$

Substitutionof Equation 2.5 in Equation 2.4 yields:

$$\frac{qB}{m} = \omega_c \qquad (2.6)$$

According to equation 2.6, the parameters that control cyclotron frequency of an ion are: the charge of the ion (q), the magnetic field strength (B) and the mass of the ion (m). In the 3 Tesla FT-ICR used in this research, B was fixed, and as a result, the cyclotron frequency depended on the mass-to-charge ratio (m/z) of the ions; the larger m/z, the smaller the ion's cyclotron frequency.

If an ion moves parallel to the magnetic field, it experiences no force from the field. The cyclotron motion only confines an ion in the x-y plane. In order to confine the ion in the z-axis, a small DC voltage (+2V) was applied to the trapping plates. This DC voltage created a parabolic potential well which prevented the ions from drifting out of the cell from two ends. The harmonic oscillation of ions along the magnetic field axis between the trapping plates is called trapping motion.[5,23] The frequency of this motion is described in the following equation:

$$\omega_t = \sqrt{\frac{2qV_t\alpha}{md^2}} \qquad (2.7)$$

where V_t is the trapping voltage, d the distance between the trapping plates and α the cell geometry constant (for a cubic cell, α = 2.77373) (Figure 2.4).

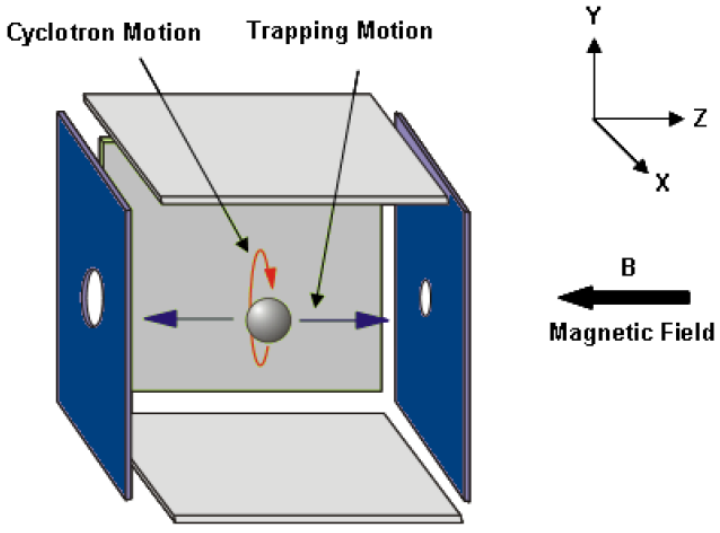

Figure 2.4 Cyclotron and trapping motions of an ion in an ICR cell

The existence of magnetron motion is due to both magnetic field and electric filed. This motion is independent of the mass of the ion. The radial force generated by the trapping potential pushes the ions radially away from the center of the cell, causing the cyclotron orbit of the ions to shift off the z-axis. The following equation shows the frequency of this motion:

$$\omega_m = \frac{2\alpha V_t}{d^2 B} \qquad (2.8)$$

where in V_t is trapping voltage, α is the geometry of the cell, d is the distance between the trapping plates, and B is the magnetic field.[24] The magnetron frequencies (1-100 Hz) are much lower than the cyclotron frequencies (5 kHz- 5MHz), and as a result, the magnetron motion does not interfere with the detection of cyclotron motion. However, the magnetron motion is an undesirable motion in the FT-ICR; it can have negative effects on ion transfer event, resolution, sensitivity, and mass accuracy.[25]

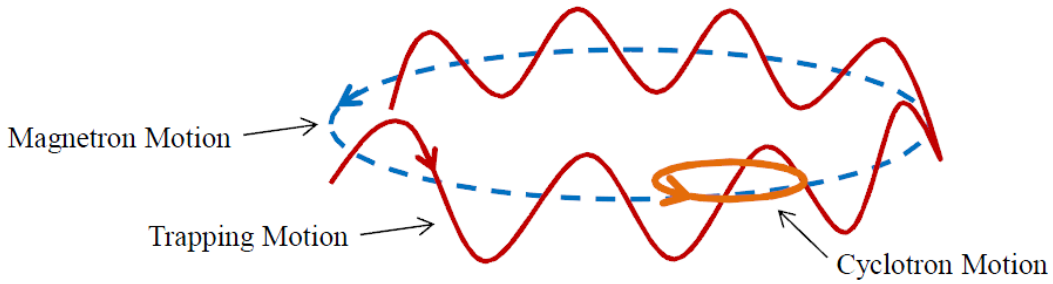

Figure 2.5 All three motions of ions in an ICR cell: cyclotron motion (orange), trapping motion (red), and magnetron motion (blue). The magnetron motion radius is greatly exaggerated comparing to the cyclotron motion in order to show them in the same figure.

2.3.3 Ion Generation

The precursors of mono- and biradicals were introduced into the instrument by a solids probe, followed by the self-CI process described above (Section 2.2.2). Ionization times varied from 1-10 s depending on the precursors.

2.3.4 Ion Transfer from Source Cell Into Analyzer Cell

Ion generation occurred in source cell of the FT-ICR. Precursor ions were transferred into analyzer cell and subjected to radical generation and ion-molecule reactions. To transfer ions from source into analyzer cell, conductance limit was grounded, the voltage on source trapping plate changed from +2 V to +2.1 V, and the voltage on analyzer trapping plate changed from +2 V to +1.9 V. As a result, the ions moved through the 2-mm hole in the conductance limit from source into analyzer cell. Transfer time ($t_{transfer}$) is dependent on the m/z of the ion, as described by the following equation:

$$t_{transfer} = 10\mu s\sqrt{m/z} \quad (2.9)$$

After transfer event, all trapping plates' (including conductance limit) voltage were set back to +2V. To reduce the energy the ions gained during the transfer process, 1-5 s cooling time was used. Ions collided with neutral molecules in the gas phase during the

cooling time, which reduced their kinetic energies, and excess internal energy was released as infrared photons.[26,27]

2.3.5 Ion Excitation and Detection

In an FT-ICR, ion generation, manipulation and detection all occur in the cell but at different times. When the experimental sequence enters the excitation and detection events, the ions are still in the cell until they are quenched.

Normally, ions' cyclotron radii are very small when trapped in the cell, and in order to be detected by the detection plates, the ions need to move on a larger orbit so that they can travel close enough to the detection plates to induce current on the plates (Figure 2.6).[28] Therefore, the ions must be excited to larger cyclotron orbits before detection. For ion excitation, a sinusoidal voltage was applied to the excitation plates. The applied radiofrequency (rf) will resonant with the cyclotron frequency of the ions.The ions absorbed energy from the field and got excited to a larger radius. The final radius of the ions' motion depends on the duration of the excitation pulse. In order to detect many different mass ions simultaneously in FT-ICR, a rapid frequency sweep[29,30] or RF chirp that covers a range of frequencies can be used.

After excitation, all the ions with the same m/z traveled as a coherent ion packet. When this packet passed one of the two detection plates, it generated a differential

current between the detection plates, called the image current.[6]The frequency of the image current is equal to the ions' cyclotron motion frequency, and the amplitude of the current is proportional to the number of ions in the packet. The initial signal from the detection plates is a time domain signal, and by using a Fourier transformation, a frequency domain spectrum can be generated from the time domain signal. A mass spectrum can be obtained by applying Equation 2.6 to the frequency domain spectrum.

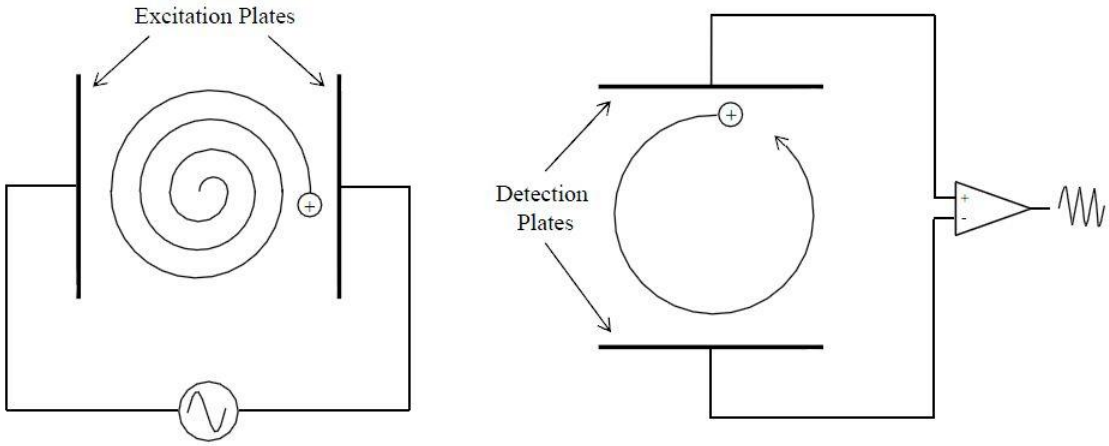

Figure 2.6 Illustration of ion excitation and detection. An rf pulse is applied to the excitation plates to increase the radius of ion cyclotron motion (left, excitation), and the induced image current is detected by the detection plates (right, detection).

As described above, the more accurate measurement of the cyclotron frequencies of the ions, the higher the resolution. Therefore, to increase the resolving power, a longer detection time is preferred. However, there is a limitation for the length of recording,

because collisions between ions and neutral atoms and/or molecules destroy the coherence of the ion packet; the longer the recording time, the more collisions occur. Thus, high vacuum is required in FT-ICR to reduce the number of unwanted collisions.

2.3.6 Ion Isolation

The basic technique of ion isolation is similar to excitation and detection; unwanted ions were removed from the cell by kinetically exciting these ions to increase their cyclotron motion radii to be larger than the size of the cell, so that these ions collided with the cell walls and got quenched. An rf sweep (Chirp) and stored waveform inverse Fourier transform (SWIFT) are two commonly used methods to remove unwanted ions.[5,6] Chirp excitation excites a broad range of frequencies to remove all ions with frequencies within this frequency range. It is fast and easy, however, it suffers from tailing at the two ends of the excitation range, which may result in the excitation of ions outside the wanted range. Also, the amplitude over the range varies in an uncontrollable manner for each ion.[6]

SWIFT excitation does not have above disadvantages because by using SWIFT, only the chosen ions are ejected and the amplitude of each excitation can be controlled. To perform SWIFT, first the frequencies which should be excited according to the m/z of the unwanted ions are determined. The amplitude of each frequency signal can be set to

required values. Time domain SWIFT waveform is obtained by conversion of the frequency domain spectrum via Fourier transform. When the SWIFT waveform is applied, all unwanted ions are simultaneously excited and ejected. In this work, chirp excitation was used for detection only and SWIFT waveform was used to isolate ions.

2.3.7 Collision-Activated Dissociation (CAD)

Ion fragmentation is a very important event in FT-ICR mass spectrometer. It allows one to either get more structural information of the analyte or synthesize radical ions in the instrument. The most commonly used method in FT-ICR is to accelerate the ion and allow it to collide with neutral atoms or molecules (collision-activated dissociation or CAD).[31] During CAD, ions are excited to gain kinetic energy, which can be partially converted into internal energy upon collisions with neutral atoms (argon was used in this work). When the activation energy is greater than the dissociation threshold, fragmentation of the ions occurs.

CAD proved not to be useful for radical generation in this work. It caused the ions to move to a larger cyclotron radius, which reduced the detection efficiency. In order to avoid this, sustained off-resonance irradiation collision-activated dissociation (SORI-CAD) was used.[32] SORI-CAD uses an rf voltage that is 1000 Hz off resonance from the cyclotron frequency of the aimed ion. So the excited ion's cyclotron radius will

periodically increase and decrease in the cell and the ion will gain lower kinetic energy than in an on-resonance process, which keeps the ions closer to the center of the cell. Meanwhile, during SORI-CAD, ions' internal energy increases slower than in the on-resonance CAD process, which results in dissociation along the lowest energy pathway, such as a homolytic cleavage of C-I or C-NO_2 bond used to generate radical site in this work.

2.4 References

1. Gross, J. H. *Mass Spectrometry*, Springer: New York, **2004**.

2. Cooks, R. G.; Wong, P. S. H. *Acc. Chem. Res.* **1998**, *31*, 379.

3. Marshall, A. G.; Comisarow, M. B.; Parisod, G. *J. Chem. Phys.* **1979,** *71*, 4434.

4. Comisarow, M.; Marshall, A. G. *Chem. Phys. Lett.* **1974,** *25*, 282.

5. Marshall, A. G.; Hendrickson, C. L.; Jackson, G. S. *Mass Spectrom. Rev*. **1998**,*17*, 1.

6. Amster, I. J. J. *Mass Spectrom.* **1996**, *31*, 1325.

7. Dempster, A. *J. Phys. Rev.* **1918**, *11*, 316.

8. Mark, T. D. *Int. J. Mass Spectrom. Ion Phys.* **1982**, *45*, 125.

9. Mark, T. D. *Electron Impact Ionization in Gaseous Ion Chemistry and MassSpectrometry*; John Wiley and Sons: New York, **1986**.

10. Vestal, M. L. *Chem. Rev.* **2001**, *101*, 361.

11. Munson, M. S. B.; Field, F. H. *J. Am. Chem. Soc.* **1966**, *88*, 2621.

12. Munson, M. S. B. *Int. J. Mass Spectrom.* **2000**, *200*, 243.

13. Cassady, C. J.; Carr, S. R. *J. Mass Spectrom.* **1996**, *31*, 247.

14. Sannes, K. A.; Brauman, J. I. *J. Phys. Chem.* **1996**, *100*, 7471.

15. Andrade, P. B. M.; Riveros, J. M. *J. Mass Spectrom.* **1996**, *31*, 767.

16. Marshall, A. G.; Wang, T. C. L.; Ricca, T. L. *J. Am. Chem. Soc.* **1985**,
17. *107*, 7893.

18. Singleton, J. H. *J. Vac. Sci. Technol. A* **2001**, *19*, 1712.

19. Carlin, T. J.; Freiser, B. S. *Anal. Chem.* **1983**, *55*, 571.

20. Dunn, W. G.; Hooper, J. B. *Anal Lett.* **1973**, *6*, 1.

21. Littlejohn, D. P.; Ghaderi, S. US Patent 4,581,533, **1986**.

22. Hofstadler, S. A.; Laude, D. A. *J. Am. Soc. Mass Spectrom.* **1990**, *1*, 351.

23. Cooper, H. J. In *Practical Aspects of Trapped Ion Mass Spectrometry*; March, R. E., Todd, J. F. J., Eds.; CRC Press: Boca Raton, **2010**, p 122.

24. Rempel, D. L.; Huang, S. K.; Gross, M. L. *Int. J. Mass Spectrom. IonProcesses* **1986**, *70*, 163.

25. Dunbar, R. C.; Chen, J. H.; Hays, J. D. *Int. J. Mass Spectrom. IonProcesses* **1984**, *57*, 39.

26. Vartanian, V. H.; Laude, D. A. *Int. J. Mass Spectrom.* **1998**, 178, 173.

27. Dunbar, R. C. *J. Chem. Phys.* **1989**, *90*, 7369.

28. Dunbar, R. C. *Mass Spectrom. Rev.* **1992**, *11*, 309.

29. Marshall, A. G.; Roe, D. C. *J. Chem. Phys.* **1980**, *73*, 1581.

30. Comisarow, M. B.; Marshall, A. G. *Chem. Phys. Lett.* **1974**, *26*, 489.

31. Marshall, A. G.; Roe, D. C. *J. Chem. Phys.* **1980**, *73*, 1581.

32. Cody, R. B.; Burnier, R. C.; Freiser, B. S. *Anal. Chem*. **1982**, *54*, 96.

33. Gauthier, J. W.; Trautman, T. R.; Jacobson, D. B. *Anal. Chim. Acta***1991**, *246*, 211.

CHAPTER 3:
A BRACKETING METHOD FOR PROTON AFFINITY (PA) MEASUREMENTS OF DEHYDRO- AND DIDEHYDROPYRIDINES

3.1 Introduction

Aromatic mono- and biradicals have received more attention in recent years because of the importance of these reaction intermediates in many fields, including the function of some antitumor and antiviral drugs.[1,2] A better understanding of the properties of radicals would facilitate the design of synthetic versions of these drugs.

Our group has studied charged mono- and biradicals in the gas phase for several years. Some of them have been found to be strong Bronsted acids. Proton affinities can be used to facilitate the identification of the structures of molecules. In order to be able to predict when proton transfer reactions are expected, gas-phase proton affinity values are needed.

Proton affinity (PA) is a fundamental property that is related to the structure andreactivity of a molecule. The proton affinity, of an anion or of a neutral atom or molecule is the energy released in the following reactions[3]:

$$A^- + H^+ \rightarrow HA$$

$$B + H^+ \rightarrow BH$$

Scheme 3.1 Definition of proton affinity

The higher the proton affinity, the stronger the base and the weaker the conjugate acid.

Unfortunately, very few experimental PA values are available for organic radicals, and none for biradicals.[5] Many experimental methods exist for the determination of proton affinities, such as the equilibrium method[5] and the Cooks' kinetic method.[6] However, the equilibrium method requires the establishment of an equilibrium between the radical and a reference base or acid. On the other hand, Cooks' kinetic method requires formation of a proton bonded dimer between the radical and a reference base or acid. Neither method can be used for proton affinity measurements of radicals due to thevery high reactivity of radicals. Another method to determine PAs is the bracketing method.[7] This method is very versatile; it is based on reactions of different reference bases with known proton affinities with the protonated radical and monitoring the occurrence of exothermic proton transfer to determine the upper and lower limits of proton affinity of the radical. However, any extra energy in the protonated radicals, such as that deposited upon collisional activation when the radical sites are generated in the precursor ions upon CAD, may cause endothermic proton transfer reactions to occur,

albeit slowly. Their occurrence limits the accuracy of the traditional bracketing measurement. Thus, a new method is needed to accurately determine PAs of radicals. We modified the bracketing method to allow us to distinguish between exothermic and endothermic proton transfer reactions. As a result, accurate proton affinities can be obtained. This method can also guide theorists as to what level of theory is best for calculating these values.

3.2 Experimental Details

All experiments were carried out using a Finnigan model FTMS 2001 Fourier transform ion cyclotron resonance mass spectrometer (FT-ICR) as described in Chapter 2. This instrument contains a differentially pumped dual cell placed within the magnetic field produced by a 3.0 T superconducting magnet operated at ca. 2.7 T. The two cells are separated by a common plate (the conductance limit) that has a 2-mm hole in the center. This plate and the other two trapping plates were kept at +2 V unless otherwise stated. The nominal base pressure in each cell ($<1\times10^{-9}$Torr) was maintained by two Edwards (Sanborn, NY, USA) diffusion pumps (800 L/s), each backed with an Alcatel mechanical pump. The pressure was measured with two Bayard-Alpert ionization gauges located on each side of the dual cell.

Generation of the (bi)radicals involved protonation of a substituted pyridine

precursor via chemical ionization (or self-CI) as described previously.[8] The pyridine precursor ions were then transferred into the other cell by grounding the conductance limit plate. The transfer time varies according to the mass of the ions being transferred, being usually between 100-160 μs as discussed in chapter 2. In the second cell, protonated (bi)radicals were generated by subjecting the precursor ions to sustained off-resonance irradiation collision-activated dissociation (SORI-CAD).[9] SORI-CAD experiments utilized off-resonance excitation of the isolated ion at a frequency ±1000 Hz of the cyclotron frequency of the ion. The number of SORI-CAD events depended on the specific radical precursors used. Mostmonoradicals were subjected to one SORI-CAD process whilebiradicals needed two. Stored-waveform inversed Fourier transform[10,11] (SWIFT), excitation was used to isolate desired ions by ejecting all unwanted ions from the cell. After isolation, the pyridinium (bi)radicalcations were allowed to interact with reference bases (Figure 3.1). Before reactions, either one or five second cooling time was used in order to reduce the energy of the (bi)radical cations via IR emission and collisions with Ar gas which was pulsed into the cells by using pulsed valves. Observation of proton transfer reaction indicates that the PA of the reference base is higher than that of the conjugate base of the (bi)radicalcation, if only exothermic reactions are assumed to occur (Figure 3.1).

Figure 3.1 Flow chart of the experiment, starting with the generation of protonated 2-dehydropyridine and transfer into another cell followed by SORI-CAD, cooling, and reaction with a reference base.

In above experiments, the concentration of the neutral reagent is much greater than that of the ions. Hence, the reactions studied here follow pseudo first-order kinetics. The second-order rate constant (k) of each ion-molecule reaction was obtained from a semi-logarithmic plot of the relative abundance of the reactant ion versus time.[12]

Error of the PA measurement can be estimated from the uncertainty of the PAs of the reference bases and the estimated error of the measurement. Error due to the brackeing is the lowest detectable endothermicity, which was determined to be $\pm$1.6 kcal/mol by examining three reactions between pairs of reference bases with known PAs (Table 3.1). This determines the minimum difference of proton affinities that can be distinguished by proton transfer reactions. If the proton affinities are too close, there either a very slow proton transfer occurs or no proton transfer is observed. Uncertainty of reference bases' PA values obtained from the NIST database[13] is $\pm$1.9 kcal/mol. As a result, the total error of the measured PAs is estimated to be ±2.6 kcal/mol. The error of the PA values is reported to be ±3 kcal/mol, which is a commonly accepted value for the bracketing method.

Table 3.1 The Lowest Detectable Endothermicity was Measured to be 1.6 kcal/mol by Observing the Occurrence of Proton Transfer Reaction between Three Pairs of Reference Bases with Known Proton Affinities[13]

Base 1[a]	Base 2	Δ Proton affinity (difference between the PAs of base 1 and base 2)	Observation of proton transfer from base 1 to base 2
		0.4 kcal/mol	Yes
		1.6 kcal/mol	Yes (slow)
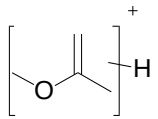 213.9 kcal/mol		1.8 kcal/mol	No

[a]Values shown under the ions are their conjugated bases' proton affinities. All proton affinities are from reference 1

3.3 Measured Proton Affinities of Dehydro- and Didehydropyridines

In traditional PA bracketing, proton transfer reactions are usually assigned to be exothermic or endothermic based on the reactions' rate constants. The rates of exothermic proton transfer reactions are assumed to be orders of magnitude greater than those of endothermic proton transfer reactions.[14] However, the common existence of parallel reaction pathways for radicals affects their reaction rates. Thus, a new approach is needed to differentiate exothermic and endothermic proton transfer reactions.

In this study, hydrogen atom abstraction reaction was found to compete with the proton transfer reactions. This reaction is not sensitive to extra internal energy in the protonated radical.[15] Hence, it can be used to distinguish exo- and endothermic proton transfer reactions since the latter reactions are highly sensitive to the protonated radical's internal energy.[15] The rate constant of the hydrogen atom abstraction was assigned to be k_1 while the rate constant of a proton transfer reaction is k_2. The ratio k_1/k_2 is given by the branching ratio of the products from the two reactions, as long as no secondary reactions are observed. Two delay times were used after generation of the radical site(s) by SORI-CAD, one and five seconds, to distinguish between exo- and endothermic proton transfer reactions. The extent of endothermic proton transfer was substantially reduced when using the longer cooling time. Hence, a fixed ratio of the two rate constants under the two different delay time conditions suggests that the proton transfer reaction is not endothermic. However, a dramatic change of this ratio or the disappearance of proton transfer products upon

the longer cooling time indicates the occurrence of an endothermic proton transfer. This was proved by the reaction between protonated 4-dehydropyridine and the reference base 2-chloropyridine. When using one second cooling time, a proton transfer reaction was observed, however, after five seconds cooling time, the proton transfer reaction was not observed. According to this method, the observed proton transfer reactions were divided into endothermic ones (indicated as no proton transfer) and exothermic ones (indicated as observation of proton transfer) in the tables provided below.

Table 3.2 Proton Affinities of 2-, 3- and 4-Didehydropyridines Measured by Observing the Occurrence of Exothermic Proton Transfer Reactions with Reference Bases

Reference Base	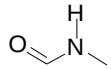			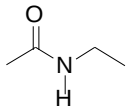				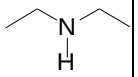
Proton Affinity[a] (kcal/mol)	203.5	210.4	212.1	214.6	215.3	215.9	217.5	227.6
	-[b]	-	+[c]	+	[d]			+
	-		-	-	+	+	+	
	-		-	-	-[e]	+	+	

[a]Reference bases' proton affinities are from reference 13 and have an uncertainty of ± 1.9 kcal/mol. [b] Negative sign indicates that an exothermic proton transfer reaction was not observed. [c] Positive sign indicates that an exothermic proton transfer reaction was observed. [d] Blank indicates that the experiment was not performed. [e] Proton transfer reaction was observed with one second cooling time but not with five seconds cooling time; hence, no proton transfer was assigned to this pair.

The proton affinities of all radicals given in the tables were measured as discussed above while employing a series of reference bases with known proton affinities (Table 3.2). The proton affinity of a radical was determined by averaging the proton affinity of the reference base with the smallest PA that abstracted a proton and of the closest reference base that did not. The experimental proton affinities obtained for 2-dehydropyridine, 3-dehydropyridine and 4-dehydropyridine are 211.3 ±3 kcal/mol, 214.9 ±3 kcal/mol and 215.6 ±3 kcal/mol, respectively.

Table 3.3 Proton Affinities of 2,3-, 2,4-, 2,5-, 2,6-, 3,4-, and 3,5-Didehydropyridines Measured by Observing the Occurrence of Exothermic Proton Transfer Reactions with Reference Bases

Reference Bases				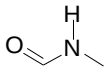			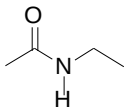		
Proton Affinity[a](kcal/mol)	191.8	194.8	198.4	203.5	207.0	212.1	214.6	215.9	217.5
			-	-[b]	+[c]	+	[d]		
				-	-	+	+		
	-	+	+	+		+			
	-	-	+	+					
				-	-	-	+	+	

Table 3.3 continued

Reference Bases				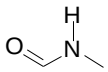			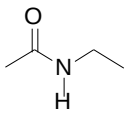		
Proton Affinity[a](kcal/mol)	191.8	194.8	198.4	203.5	207.0	212.1	214.6	215.9	217.5
				-		-	-	+	+

[a]Reference bases' proton affinities are from reference 13 and have the uncertainty of ± 1.9 kcal/mol. [b] Negative sign indicates that an exothermic proton transfer reaction was not observed. [c] Positive sign indicates that an exothermic proton transfer reaction was observed. [d] Blank indicates that the experiment was not performed

The same method was applied to measure the PAs of several didehydropyridine diradicals (Table 3.3). The experimental PA values obtained for 2,3-didehydropyridine, 2,4-didehydropyridine 2,5-didehydropyridine, 2,6-didehydropyridine, 3,4-didehydropyridine and 3,5-didehydropyridine are 205.3 ±3 kcal/mol, 209.6 ± 3 kcal/mol, 193.3 ±3 kcal/mol, 196.6 ±3 kcal/mol, 213.4 ±3 kcal/mol and 215.2 ±3 kcal/mol, respectively.

3.4 Comparison of Calculated and Experimental Proton Affinity Values

PAs of the (bi)radicals were calculated by Dr. John Nash at the RHFUCCSD(T)/cc-pVTZ//UBPW91/cc-pVDZ level of theory by using an isodesmic equation involving proton transfer to pyridine and corrected for zero-point vibrational energy differences at 298 K by using the (unscaled) UBPW91/cc-pVDZ frequencies. The experimental values are compared with the calculated values in Table 3.4. The calculated and experimental values are in an excellent agreement with two exceptions.

Table 3.4 Comparison of Calculated and Experimental PAs of the Radicals and Biradicals

(Bi)Radical									
Calculated PA (kcal/mol)	210.2	216.5	217.7	207.1	207.7	204.6[a] 190.7[b]	197.0[c] 213.5[d]	212.3	215.6
Experimental PA (kcal/mol)	211.3 ±3	214.9± 3	215.6 ±3	205.3 ±3	209.6 ±3	193.3 ±3	196.6 ±3	213.4 ±3	215.2 ±3

[a]Proton affinity of 2,5-didehydropyridine. [b] Proton affinity of ring-opened isomer. [c] Proton affinity of triplet state radical. [d]Proton affinity of singlet state radical.

Among the biradicals studied in this work, 2,5-didehydropyridine and 2,6-didehydropyridine present special cases. Protonated 2,5-didehydropyridine was never formed in FT-ICR as its precursorcation undergoes ring opening reaction upon CAD eventually to produce an enediyne isomer (Figure 3.2), according to literature.[16] Thus, the proton affinity measured here is actually the proton affinity of the enediyneisomer. This can be proven by the comparison of calculated PA values of the biradical and its ring-opened enediyne isomer and the experimentally measured PA value. Based on calculations, the proton affinities of 2,5-didehydropyridine and itsenediyne isomer are 204.6 kcal/mol and 190.7 kcal/mol, respectively. Meanwhile, from experiment, the proton affinity of 2,5-didehydropyridine was determined to be 193.3 kcal/mol which is very close to the calculated PA of theenediyne isomer. Hence, the agreement of the experimental PA value and the calculated PA value of the enediyne isomer demonstrates that the 2,5-didehydropyridium cation was not generated in the FT-ICR, and instead, its enediyne isomer was formed.

Figure 3.2 Structures of the 2,5-didehydropyridium cation (left) and its enediyne isomer (right)

Previously, the 2,6-didehydropyridinium cation has been found to show radical properties but abnormal reaction efficiencies.[17] This puzzle was solved when the proton affinity of 2,6-didehydropyridine was measured using the bracketing method discussed here. The experimental value matches the value calculated at the RHFUCCSD(T)/cc-pVTZ//UBPW91/cc-pVDZ level of theory for the triplet 2,6-didehydropyridinium cation instead of the singlet cation. (Table 3.4)

3.5 Conclusions

The modified bracketing method described here gave accurate values for proton affinities of the chosen mono- and biradicals based on the good agreement between the experimental values and those calculatedat the RHFUCCSD(T)/cc-pVTZ//UBPW91/cc-pVDZ level of theory by using an isodesmic equation involving proton transfer to pyridine. It can also be applied to measure proton affinities of other radicals/molecules whose PAs cannot be easily measured by other methods, as long as the radicals/molecules can be generated in the instrument and proper reference bases are available. In order to make a more accurate measurement, a reference reaction, such as hydrogen abstraction reaction here, is needed to check if an endothermic proton transfer occurred. Different cooling times before ion isolation and reaction helps to distinguish endothermic and exothermic proton transfer reactions.

The measured PA values demonstrate that pyridine based radicals are less basic than

pyridine itself. This is explained by the electron-deficient radical sites in the radical species.

Accurate values of proton affinities are useful when identifying the structures of mono- and biradicals. 2,5-Didehydropyridine and 2,6-didehydropyridine are two special cases. PA measurement of 2,5-didehydropyridine demonstrated that the 2,5-didehydropyridinium cation cannot be generated in FT-ICR by using the methods described in the literature.[6]The cation generated in FT-ICR was not protonated 2,5-didehydropyridine but its enediyne isomer, as the experimental PA value agrees with the PA value calculated fo the ring-opening enediyne isomer.

On the other hand, PA measurement of the 2,6-didehydropyridine demonstrated that the 2,6-didehydropyridinium cation reacts from the triplet surface.[17] The experimental PA value of 2,6-didehydropyridine agrees with the value calculated for the triplet 2,6-didehydropyridine instead of the singlet one.

3.6 References

1. Gross, J. H. *Mass Spectrometry*; Springer: New York, **2004**.

2. Cooks, R. G.; Wong, P. S. H. *Acc. Chem. Res.* **1998**, *31*, 379.

3. Bartmess, J.; Linstrom, P. J.*NIST Standard Reference Database,NIST Chemistry WebBook,* NIST, Gaithersburg, MD, **2001.**

4. DeFrees, D. J. Defrees, R. T. McIver, *J. Am. Chem. Soc.***2002**, *102,* 3334.

5. Meot-Ner, M. *Int. J. Mass. Spec.* **2003,** *227,* 525.

6. Cooks, R. G.; Kruger, T. L.*J. Am. Chem. Soc.* **1977,** *99,* 1279.

7. Chowdhury, A. K.; Wilkins, C. L. *J. Am. Chem. Soc.* **1989,** *111,* 3150.

8. Price, J. M.; Kenttämaa, H. I.*J. Phys. Chem. A.* **2003**, *107,* 8985.

9. Gauthier, J. W.; Trautman, T. R.; Jacobson, D. B.*Anal. Chim. Acta.***1991**, *246,* 211.

10. Marshall, A. G.; Ricca, T. L.*J. Am. Chem. Soc*. **1985**, *107,* 7893.

11. Amster, I. J. J. *Mass Spectrom.* **1996**, *31*, 1325.

12. Amegayibor, F. S.; Nash, J. J.; Lee, A. S.; Kenttämaa, H. I.*J. Am. Chem. Soc*. **2002**, *124,* 12066.

13. Hunter, E. P.; Lias, S. G.*J. Phys. Chem. Ref. Data.* **1998,** *27,* 413.

14. Gorman, G. S.; Amster, I. J.*Org. Mass Spec.* **1993,** *28,* 1602.

15. Kim, H.; Liu, J.; Anderson, S. L. *J. Chem. Phys.***2001**, *115,* 5843.

16. Kirkpatrick, L. M.;Vinueza, N.R.;Jankiewicz,B. J.;Gallardo,V. A.;Archibold,E. A.; Nash, J. J.; Kenttämaa, H. I.*Chem. Eur. J.***2013**, *19,* 9022.

17. Jankiewicz, B. J.; Kenttämaa, H. I. *J. Phys. Org. Chem*. **2013**, *26,* 707.